

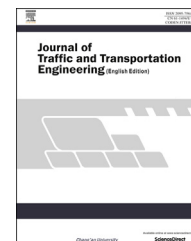
HOSTED BY



ELSEVIER

Available online at [www.sciencedirect.com](http://www.sciencedirect.com)

ScienceDirect

journal homepage: [www.elsevier.com/locate/jtte](http://www.elsevier.com/locate/jtte)

## Original Research Paper

# Analysis of transient viscoelastic response of asphalt concrete using frequency domain approach

Yanqing Zhao<sup>\*</sup>, Sajjad Yousefi Oderji, Peisong Chen

School of Transportation Engineering, Dalian University of Technology, Dalian 116024, China

## ARTICLE INFO

## Article history:

Available online 17 October 2015

## Keywords:

Asphalt concrete

Linear viscoelastic

Transient response

Fourier transformation

Aliasing

## ABSTRACT

The analysis of transient linear viscoelastic response of asphalt concrete (AC) is important for engineering applications. The traditional transient response of AC is analyzed in the time domain by performing complicated convolution integral. The frequency domain approach allows one to determine the transient responses by performing simple multiplication instead of the complicated convolution integral, and it does not require the time derivative of the input excitation, and thus, the approach could greatly reduce the analysis complexity. This study investigated the frequency domain approach in calculating the transient response by utilizing the discrete Fourier transform technique. The accuracy and effectiveness of the frequency domain approach were verified by comparing the analytical and calculated responses for the standard 3-parameter Maxwell model and by comparing the time and frequency domain solutions for AC. The effect of aliasing of the frequency domain approach can effectively reduce by selecting a small sampling interval for the time domain excitation function. A sampling interval is acceptable as long as the amplitude of the Fourier transformed excitation is close to 0 more than half of the sampling rate. The results show that the frequency domain approach provides a simple and accurate way to perform linear viscoelastic analysis of AC.

© 2015 Periodical Offices of Chang'an University. Production and hosting by Elsevier B.V. on behalf of Owner. This is an open access article under the CC BY-NC-ND license (<http://creativecommons.org/licenses/by-nc-nd/4.0/>).

## 1. Introduction

Frequency domain analysis plays an important role in many branches of engineering. By taking the Fourier transform, the differential or integral equations used to describe a physical system in the time domain are converted to algebraic equations in the frequency domain, which greatly reduces the complexity of the problem-solving process. The Fourier transform is essentially a universal problem-solving technique (Brigham,

1988), and it allows one to examine a particular relationship from an entirely different viewpoint. Furthermore, the computational efficiency can be significantly improved by taking the advantage of the fast Fourier transform (FFT) algorithm.

In pavement engineering, an important application of the frequency domain approach is to determine the complex modulus of asphalt concrete (AC) (AASHTO, 2007). In the complex modulus testing, the specimen is subjected to a

<sup>\*</sup> Corresponding author. Tel.: +86 15804269202.

E-mail addresses: [yanqing\\_zhao@dlut.edu.cn](mailto:yanqing_zhao@dlut.edu.cn) (Y. Zhao), [su\\_a\\_2006@yahoo.com](mailto:su_a_2006@yahoo.com) (S. Y. Oderji), [sdwcps@163.com](mailto:sdwcps@163.com) (P. Chen).

Peer review under responsibility of Periodical Offices of Chang'an University.

<http://dx.doi.org/10.1016/j.jtte.2015.10.003>

2095-7564/© 2015 Periodical Offices of Chang'an University. Production and hosting by Elsevier B.V. on behalf of Owner. This is an open access article under the CC BY-NC-ND license (<http://creativecommons.org/licenses/by-nc-nd/4.0/>).

cyclic haversine stress or strain excitation, and the complex modulus is determined from the steady-state response (Chehab et al., 2003; Gibson et al., 2003; Pellinen et al., 2007; Underwood et al., 2006). Theoretically, the steady-state response can only be achieved after infinite load cycles for linear viscoelastic (LVE) solid materials. However, the in-situ response caused by a moving load is far from reaching the steady-state. Instead, the response decays gradually and approaches 0 as the load moves away. Therefore, the transient response analysis is more pertinent to engineering applications (Chen et al., 2009; Elseifi et al., 2006; Wang et al., 2006; Zhao et al., 2014).

The transient LVE response of AC is conventionally analyzed in the time domain through numerical evaluation of the convolution integral. Besides the computation complexity in solving the convolution integral, analysis in the time domain requires the derivative of input excitation with respect to time, which usually causes computational difficulties when the excitation contains discontinues. These shortcomings are avoided in frequency domain approach. Researchers have used Fourier transform or Laplace transform to conduct inter-conversions of LVE functions of AC. In these studies, theoretical solutions can be derived, since the time domain functions are defined as the responses due to constant stress or strain input (Kim et al., 2008; Luo and Lytton, 2010). This study aims to investigate the frequency domain approach in analyzing transient responses of AC under arbitrary input history where the theoretical solutions are not available. Also, methods for improving the accuracy of analysis results are proposed.

## 2. Theoretical background and discrete Fourier transform

According to the Boltzmann superposition principle, the constitutive relationship of LVE materials can be expressed in the form of convolution integral as follows

$$\sigma(t) = \int_0^t E(t-\tau) \frac{\partial \varepsilon}{\partial \tau} d\tau \quad (1)$$

$$\varepsilon(t) = \int_0^t D(t-\tau) \frac{\partial \sigma}{\partial \tau} d\tau \quad (2)$$

where  $\varepsilon$  and  $\sigma$  are strain and stress, respectively,  $\tau$  is a time-like integration variable,  $t$  is time,  $E(t)$  and  $D(t)$  are relaxation modulus and creep compliance, respectively. By applying the Fourier transform to both sides of the above equations and after some mathematical manipulations, the following relations are obtained (Tschoegl, 1989).

$$\bar{\sigma}(\omega) = \bar{\varepsilon}(\omega) E^*(\omega) \quad (3)$$

$$\bar{\varepsilon}(\omega) = \bar{\sigma}(\omega) D^*(\omega) \quad (4)$$

where  $\omega$  is the angular frequency, a bar over a symbol means that the quantity has been Fourier transformed,  $E^*(\omega)$  and  $D^*(\omega)$  are complex modulus and complex compliance, respectively, and their relationship is as follow

$$E^*(\omega) = \frac{1}{D^*(\omega)} \quad (5)$$

where  $E^*(\omega)$  and  $D^*(\omega)$  are also called frequency response functions (FRF). The Fourier transform of a time domain function,  $f(t)$ , is defined as follow

$$\bar{f}(\omega) = \int_{-\infty}^{+\infty} f(t) e^{-j\omega t} dt \quad (6)$$

where  $j = \sqrt{-1}$ ,  $\bar{f}(\omega)$  is a complex function and it has real and imaginary parts.

The Fourier transformed stress–strain relationship shown in Eqs. (3) and (4) allows one to determine the viscoelastic response by performing simple multiplication in the frequency domain instead of complicated convolution in the time domain. The evaluation of Eqs. (3) and (4) involves 3 steps: (1) transform the time domain excitation to the frequency domain; (2) multiply the transformed excitation by the corresponding FRF; (3) take the inverse Fourier transform of the multiplication results to obtain the time domain response solution. The inverse Fourier transform is defined as

$$f(t) = \frac{1}{2\pi} \int_{-\infty}^{+\infty} \bar{f}(\omega) e^{j\omega t} d\omega \quad (7)$$

For real-world engineering applications, the right sides of Eqs. (3) and (4) are usually complicated (and complex) function, and the analytical solution of the inverse transform is not easily obtained. In such cases, the forward and inverse transforms need to be evaluated using discrete Fourier transform (DFT).

To use DFT, a time domain function,  $f(t)$ , is sampled to obtain a discrete-time sequence denoted by  $x(n) = (x_0, x_1, \dots, x_{N-1})$ , in which the variable  $n$  is integer-valued and represents discrete instances in time. It is noted that the index of  $x(n)$  starts at 0 indicating the first sample time is 0. The DFT of the  $N$ -point sequence,  $x(n)$ , is given by Stearns and Hush (2003).

$$X(k) = \sum_{n=0}^{N-1} x(n) e^{-j2\pi nk/N} \quad k = 0, 1, \dots, N-1 \quad (8)$$

where  $X(k)$  is a complex-valued sequence ( $X_0, X_1, \dots, X_{N-1}$ ), equally separated by  $\Delta\omega$  on the frequency axis,  $\Delta\omega$  is the frequency domain sample interval and  $\Delta\omega = 2\pi/(\Delta t N)$ . The frequency of  $X_i$  is mean  $i\Delta\omega$ . The inverse discrete Fourier transform (IDFT) of  $X(k)$  is given by Stearns and Hush (2003).

$$x(n) = \frac{1}{N} \sum_{k=0}^{N-1} X(k) e^{j2\pi nk/N} \quad (9)$$

Eqs. (8) and (9) can be efficiently evaluated through the fast Fourier transform (FFT) algorithm (Cooley and Turkey, 1965).

## 3. Analysis of standard 3-parameter Maxwell model

The standard 3-parameter Maxwell model was first analyzed to evaluate the effectiveness of the frequency domain

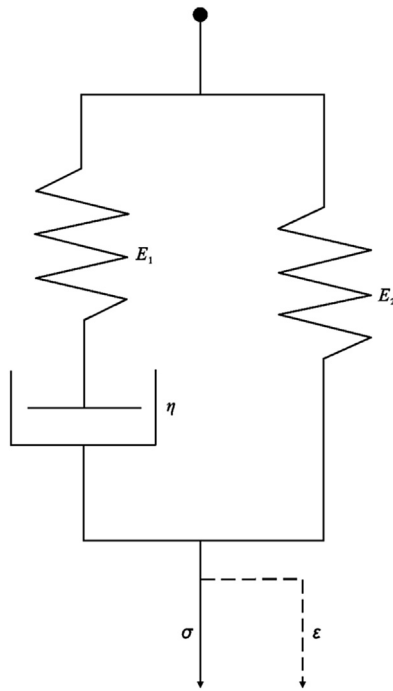


Fig. 1 – Standard 3-parameter Maxwell model.

approach in calculating LVE responses. The model is selected because it has a simple form as shown in Fig. 1, and an analytical solution can be obtained from the time domain constitutive relation shown in Eqs. (1) and (2) for some simple excitations. The analytical solution is then compared to the numerical solution obtained from Eqs. (3) and (4).

The creep compliance of the standard Maxwell model is given by Tschoegl (1989).

$$D(t) = \frac{1}{E_g} + \frac{E_g - E_2}{E_g E_2} (1 - e^{-t/\tau'}) \quad (10)$$

where  $E_g = E_1 + E_2$ ,  $\tau' = E_g \eta / (E_1 E_2)$ ,  $E_1$  and  $E_2$  are stiffnesses of the springs, respectively,  $\eta$  is the coefficient of viscosity of the dashpot. In this study,  $E_1 = 1000$  MPa,  $E_2 = 50$  MPa, and  $\eta = 250$  MPa·s. The model is subjected to a creep and recovery test in which a constant stress level,  $\sigma_0$ , is applied instantaneously to the model at the beginning of the test, and the stress is hold for a duration of  $t_0$  and then removed. According to the superposition principle, the loading sequence can be expressed as

$$\sigma(t) = \sigma_0 H(t) - \sigma_0 H(t - t_0) \quad (11)$$

where  $H(t)$  is the Heaviside step function. By substituting Eqs. (10) and (11) into Eq. (1), the strain response is easily obtained as follow

$$\varepsilon(t) = \sigma_0 D(t) - \sigma_0 D(t - t_0) \quad (12)$$

In this study,  $\sigma_0 = 0.1$  MPa and  $t_0 = 5$  s. The analytical strain response, as well as the loading sequence, is presented in Fig. 2.

The complex modulus of the standard Maxwell model is given by Tschoegl (1989).

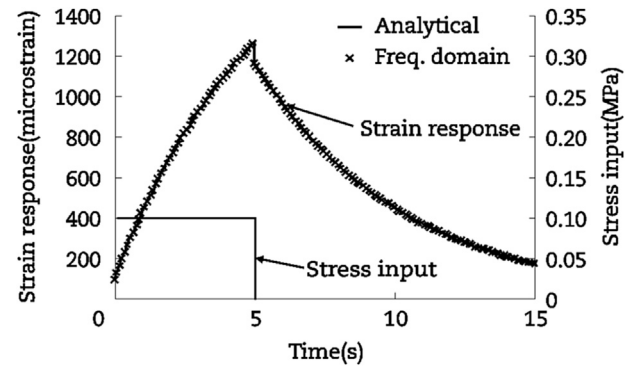


Fig. 2 – Strain responses obtained using different approaches for standard Maxwell model.

$$E^*(\omega) = E_2 + E_1 \frac{i\omega\tau}{1 + i\omega\tau} \quad (13)$$

where  $\tau = \eta/E_1$ . Although the analytical form of Fourier transform of the stress excitation in Eq. (11) is available (Bracewell, 2000), the inverse Fourier transform of the right side of Eq. (2) is difficult. The discrete approach utilizing FFT as discussed previously was employed to compute the strain response. The frequency domain solution is also presented in Fig. 2. It is seen that the frequency domain solution is in good agreement with the time domain analytical solution, indicating the frequency domain approach is effective in calculating LVE transient responses. Detailed analysis procedures are presented in the subsequent sections.

#### 4. Transient response analysis of AC

A complex modulus model of AC is needed to analyze LVE responses of the material using the frequency domain approach. It has been shown that the modified Havriliak–Negami (MHN) model can accurately characterize the LVE properties of AC in the complex domain (Zhao et al., 2013).

$$E^*(\omega) = E_{0HN} + \frac{E_{\infty HN} - E_{0HN}}{[1 + (\omega_0/i\omega)^\alpha]^\beta} \quad (14)$$

where  $E_{\infty HN}$  and  $E_{0HN}$  are complex moduli as  $\omega$  approaches  $\infty$  and 0, respectively,  $\alpha$ ,  $\beta$  and  $\omega_0$  are model coefficients,  $\alpha$  and  $\beta$  are associated with relaxation mechanisms,  $\omega_0$  is related to time-temperature shifting and controls the horizontal positions of response function master curves. The model coefficients determined by Zhao et al. (2013) for a SMA 12.5 mixture, as shown in Table 1, were used in this study.

Table 1 – Coefficients of complex modulus model used in analyses.

$E_{\infty}$ (MPa)	$E_0$ (MPa)	$\alpha$	$\beta$	$\omega_0$
26,317	51.1	0.266	1.693	657.1

#### 4.1. Transient and steady-state responses

The haversine function, as shown in Eq. (15), is widely used to represent the stress pulse caused by a moving load (Al-Qadi et al., 2008; Huang, 2003).

$$\sigma(t) = A \sin^2\left(\frac{\pi t}{d}\right) = A \left[ \frac{1}{2} + \frac{1}{2} \sin\left(\frac{2\pi t}{d} - \frac{\pi}{2}\right) \right] \quad (15)$$

where  $d$  is the stress duration,  $A$  is the stress amplitude.

Eq. (15) was used in this study to produce the stress excitation. It is seen that the haversine function consists of a constant stress ( $A/2$ ) and a sinusoid. Since both the forward and inverse Fourier transforms are linear (Bracewell, 2000), the evaluation of Eq. (2) can be performed on the constant part and the sinusoidal part separately, and the solutions obtained for the two parts are then combined to get the total response. For the constant part, the Fourier transform of  $A/2$  is  $A\delta(\omega)/2$ , and  $\delta(\omega)$  is the Dirac delta function (Brigham, 1988). Because the complex compliance is the reciprocal of the complex modulus as shown in Eq. (5), the strain response is the inverse Fourier transform of  $A\delta(\omega)/(2E_0)$ , which is  $A/(2E_0)$ . Therefore, the response to a constant stress is a constant strain. Similar derivations can be made for the sinusoidal part. The strain response to a sinusoidal stress with a frequency of  $\omega_a$  is also a sinusoid with the same frequency. The ratio of the amplitude of the strain sinusoid to that of the stress sinusoid is equal to the absolute value of complex compliance at  $\omega_a$ , and the phase angle of the strain sinusoid is equal to that of the stress sinusoid minus that of complex compliance at  $\omega_a$ . Therefore, the total strain response to the stress excitation in Eq. (15) is a sinusoid plus a constant strain level.

It is worth noting that the above derivations and results are true only when  $t \in (-\infty, +\infty)$ . If the input excitation is 0 for  $t < 0$ , the total response consists of transient response and steady-state response. However, as  $t \rightarrow +\infty$ , the transient response tends to 0, and the total response approaches the steady-state response that is the solution derived above. Actually, for the problem at hand, there should be a loading time constraint,  $t \in (0, d)$ , in Eq. (15). For viscoelastic solid materials, the total response under such a loading condition decays gradually and approaches 0 eventually, therefore, the total response is the transient response.

#### 4.2. Analysis procedures of frequency domain approach

The first step in determining the transient response using the frequency domain approach is to form a discrete sample sequence of the stress input in Eq. (15) with the time constraint,  $t \in (0, d)$ . In this study, the parameters in Eq. (15),  $A$  and  $d$ , were chosen to be 0.15 MPa and 1 s, respectively. The loading pulse was sampled at an interval of 0.05 s. The FFT was then taken on the stress sample sequence (length  $N$ ) producing a discrete complex number sequence of the same length ( $X_0, X_1, \dots, X_{N-1}$ ). The real and imaginary parts of the transformed results are presented in Fig. 3. The  $N$  complex numbers are sufficient to define the DFT since the values of DFT outside this range of  $N$  are repetitive. In other words, the DFT is a periodic complex function with a period of  $N$  samples. Furthermore,  $X_{N-i}$  is the complex conjugate of  $X_i$ .

Thus, all the independent values of DFT are  $X_0, X_1, \dots, X_{N/2}$  (Stearns and Hush, 2003) and they are plotted in Fig. 3. It is seen that the DFT of the stress sample sequence spreads over a range of frequencies and approaches 0 at large frequencies. The DFT of a sinusoid with a frequency of  $\omega_a$ , and infinite duration consists of a component at 0 frequency and 2 components at  $\pm\omega_a$  in one period. The difference in the DFT results leads to the transient and steady-state responses.

Once the DFT of the stress sample sequence was determined, the components of the DFT were multiplied by the complex compliances at the corresponding frequencies to get the DFT of the strain response. The complex compliances were computed according to Eqs. (5) and (14). The IDFT was then taken on the multiplication results, and real number  $N$  was obtained which was the strain response in the time domain, as shown in Fig. 4.

For comparison purpose, the response was also computed numerically using the time domain approach according to Eq. (1). To this end, the creep compliance,  $D(t)$ , and relaxation modulus,  $E(t)$ , need to be determined from the complex modulus model. The Prony series representations of  $E(t)$  and  $D(t)$  are as follows

$$E(t) = E_\infty + \sum_{m=1}^M E_m \exp(-t/\rho_m) \quad (16)$$

$$D(t) = D_0 + \sum_{m=1}^M D_m [1 - \exp(-t/\tau_m)] \quad (17)$$

where  $\rho_m$  and  $\tau_m$  are relaxation time and retardation time, respectively,  $E_m$  and  $D_m$  are Prony series coefficients,  $E_\infty$  and  $D_0$  are equilibrium relaxation modulus and initial creep compliance, respectively. The conversion from frequency domain functions to time domain functions is based on the following LVE relations (Tschoegl, 1989).

$$E'(\omega_n) = E_\infty + \sum_{m=1}^M \frac{\omega_n^2 \rho_m^2 E_m}{\omega_n^2 \rho_m^2 + 1} \quad n = 1, \dots, N \quad (18)$$

$$D'(\omega_n) = D_0 + \sum_{m=1}^M \frac{1}{\omega_n^2 \tau_m^2 + 1} D_m \quad n = 1, \dots, N \quad (19)$$

where  $E'$  and  $D'$  are storage modulus and storage compliance, respectively. The analytical forms of  $E'$  and  $E''$  of the MHN model in Eq. (14) are documented elsewhere (Zhao et al., 2013). The storage compliance is given as below

$$D' = \frac{E'}{E^2 + E'^2} \quad (20)$$

The time domain and complex domain viscoelastic constants are related as below (Tschoegl, 1989).

$$E_\infty = E_{0HN}, \quad D_0 = \frac{1}{E_{\infty HN}} \quad (21)$$

The Prony series coefficients were determined according to Eqs. (18)–(21) using the collocation method (Park and Kim, 2001; Park and Schapery, 1999; Tschoegl, 1989). The results are presented in Table 2. The convolution integral in Eq. (1) was computed numerically using the piecewise linear approach

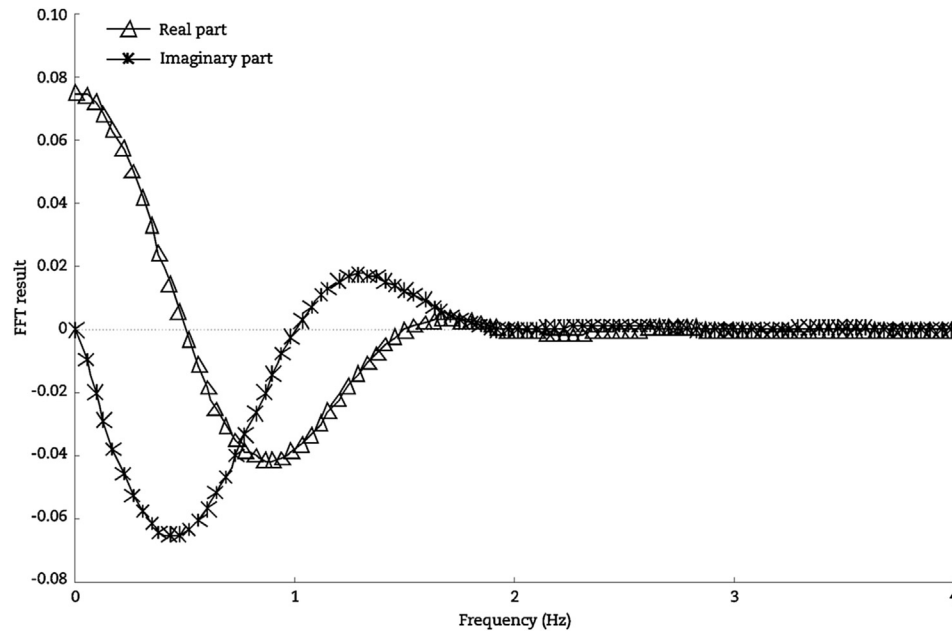


Fig. 3 – FFT results of stress excitation.

in which the input history was divided into small segments and the input was assumed to vary linearly in each segment. The time derivative of the input in Eq. (1) was obtained using the central difference equation, and the convolution integral was evaluated using the trapezoidal rule.

The strain response obtained from the time domain approach is also presented in Fig. 4. The figure shows good agreement between the results obtained from the frequency and time domain approaches. To further validate the frequency domain approach, the same analysis was performed on a haversine strain input. The amplitude of the

strain excitation is  $100 \mu\epsilon$  and the duration is 1 s. The results obtained from the two approaches are presented in Fig. 5. The results indicate that the frequency domain approach is effective in analyzing the transient LVE response for both stress and strain excitations.

The frequency domain approach can greatly enhance the computational efficiency by taking advantage of FFT technique. It takes less than 0.2 s to calculate the responses shown in Figs. 4 and 5 on a computer with Intel i5 CPU, while it takes about 2.3 s for the time domain approach. By using the frequency domain approach, the partial differential equations,

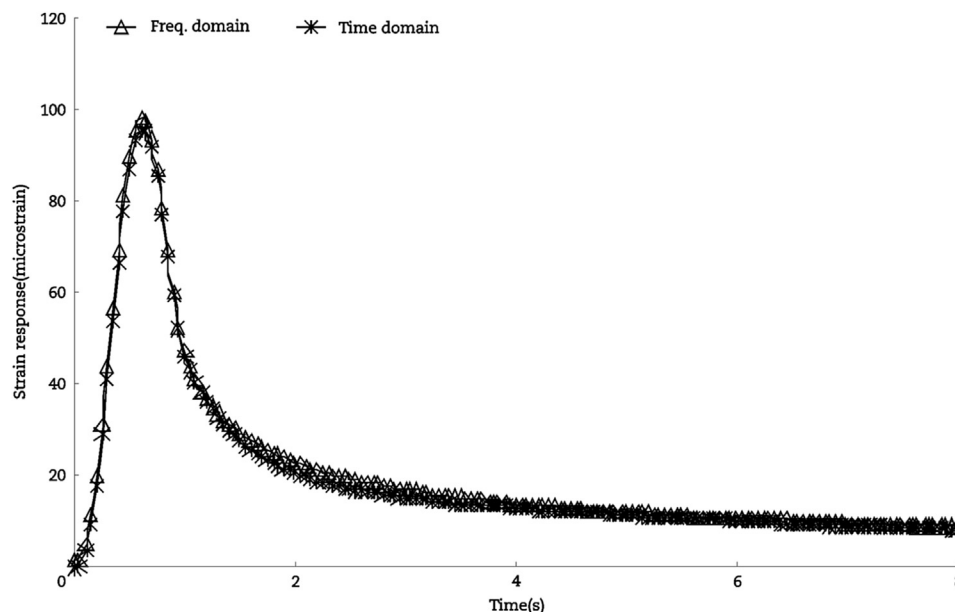


Fig. 4 – Strain responses obtained using different approaches for asphalt concrete.



**Table 2 – Prony series coefficients of  $E(t)$  and  $D(t)$ .**

Item	$E(t)$		$D(t)$	
	$\rho_m$	$E_m$	$\tau_m$	$D_m$
1	1E-06	2678.020000	5E-07	1.05E-05
2	1E-05	3923.623000	5E-06	6.63E-06
3	1E-04	4924.171000	5E-05	1.68E-05
4	1E-03	4736.239000	5E-04	3.38E-05
5	1E-02	3315.098000	5E-03	7.44E-05
6	1E-01	1758.013000	5E-02	1.74E-04
7	1E+00	780.728700	5E-01	4.29E-04
8	1E+01	307.797800	5E+00	10.91E-04
9	1E+02	118.981500	5E+01	26.82E-04
10	1E+03	40.506290	5E+02	51.73E-04
11	1E+04	17.613580	5E+03	54.32E-04
12	1E+05	3.288208	5E+04	27.70E-04
13	1E+06	4.146046	5E+05	10.67E-04
	$E_\infty$	51.1	$D_0$	3.80E-05

which govern the behavior of pavement structures under traffic loading, can reduce to simple algebra equations in the transformed domain. Thus the responses of structures can be easily determined in the transformed domain and then the time domain solutions can be obtained by taking the inverse transform. The frequency domain approach provides an effective way of analyzing responses of pavement structures.

#### 4.3. Aliasing effects

It is noted that both the frequency and time domain approaches presented above are approximate methods. The errors of the time domain approach are caused by: (1) Prony series representation of  $E(t)$  or  $D(t)$  determined using the collocation method (Tschoegl, 1989); (2) time derivative of the input excitation; (3) numerical integration. The accuracy can be improved by reducing integral intervals. For the frequency domain approach, the errors can be caused by

aliasing. According to the theory of Fourier transform, the time domain sampling results in frequency domain convolution. The Fourier transform of the time domain sampling function,  $\psi(t)$ , is the frequency domain sampling function,  $\zeta(f)$ . If the time domain sampling interval,  $\Delta t$ , is too large, the equidistant impulses of  $\zeta(f)$  would become more closely spaced, and thus, the convolution in the frequency domain may result in overlap. This distortion of the desired Fourier transform of a sampled function is called aliasing (Brigham, 1988). When aliasing occurs, the time domain samples will not exactly contain the same information as the original function. The sampling theorem states that if a continuous function,  $f(t)$ , is sampled at a rate greater than twice of its highest frequency component,  $f_c$ , then  $f(t)$  can be uniquely determined from its samples, or in other words, the samples and  $f(t)$  can contain exactly the same information.

For the sampling theorem to hold,  $f(t)$  must be band-limited or the Fourier transform of  $f(t)$  must be 0 for frequencies larger than  $f_c$ , which is the bandwidth of  $f(t)$ . However, the stress curve caused by a moving load is of finite duration and it can not be band-limited (Brigham, 1988), and thus, sampling must result in aliasing. Therefore, it is important to choose a sample interval that is small enough, so that aliasing will be kept within an acceptable range. Recall that Fig. 3 presents the Fourier transform results of the haversine stress function in Eq. (15) with the time constraint,  $t \in (0, d)$ . The function was sampled at an interval of 0.05 s meaning the resulting samples contained no frequency component over 10 Hz. It is seen from Fig. 3 that the contents of FFT are close to 0 when frequencies are larger than 2 Hz. Therefore, the 0.05 s interval resulted in minimal aliasing and produced accurate results as shown in Fig. 4.

To further illustrate the effects of aliasing, a typical 3-layer asphalt pavement was analyzed using finite element model in which the top asphalt layer was treated as linear viscoelastic. The vertical compressive stress curve in the asphalt layer obtained from the analysis is present in Fig. 6 inset. The shape

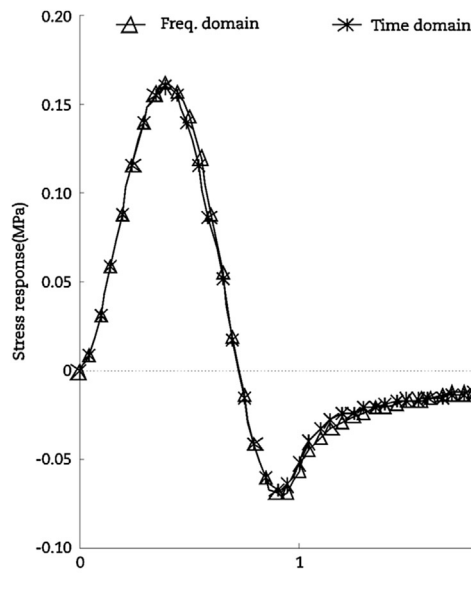


**Fig. 5 – Stress responses obtained using different approaches for asphalt concrete.**

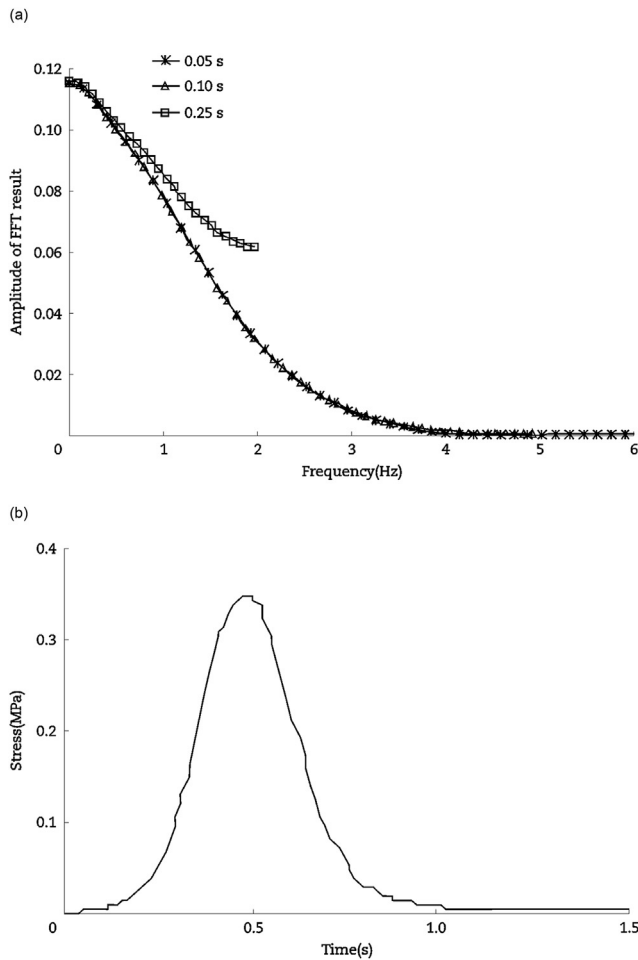


**Fig. 6 – Amplitude spectra obtained at different sample intervals. (a) FFT-frequency curve. (b) Stress-time curve.**

of the computed stress curve is similar to that measured at the Virginia Smart Road (Al-Qadi et al., 2008). The stress curve was sampled using 3 different intervals, namely 0.05, 0.10 and 0.25 s, and then the FFT was taken on the 3 sets of samples. The plots of the amplitudes of the FFT results versus

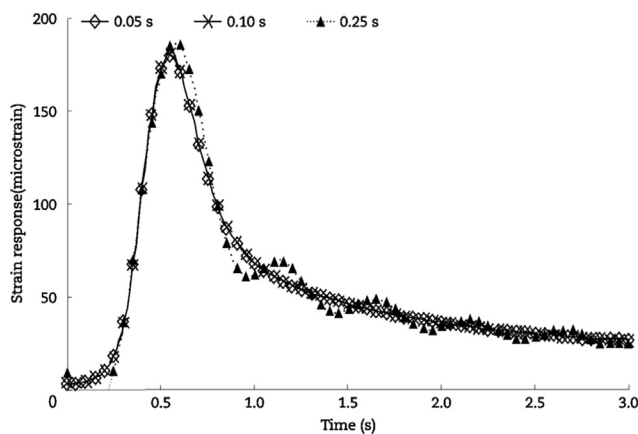


**Fig. 7 – Strain responses obtained at different sample intervals.**

frequency, also called amplitude spectra, are shown in Fig. 6. It is seen that 0.05 and 0.10 s intervals produce minimal aliasing since the FFT contents of the stress curve over half of the sampling rates are close to 0. However, significant aliasing is observed for the 0.25 s interval. The strain responses obtained from the 3 sample sets are presented in Fig. 7. The figure shows that the aliasing causes significant errors in the strain response for the 0.25 s interval. Therefore, it is important to select a small sample interval so that the aliasing effect is negligible. To this end, the amplitude spectrum of the excitation FFT result needs to be examined to ensure that the amplitude is close to 0 when frequencies are larger than half of the sampling rate.

## 5. Conclusions

In this study, the LVE response of AC was analyzed in the frequency domain using the discrete Fourier transform technique. The frequency domain approach was verified by comparing the analytical and computed responses for the standard 3-parameter Maxwell model and by comparing the time domain and frequency domain solutions for AC, which was characterized using the MHN model. The results show that the frequency domain approach is accurate and effective in analyzing the LVE transient responses of AC. It allows one to determine the LVE responses by performing simple multiplication in the frequency domain instead of complicated convolution in the time domain, and it does not require the time derivative of the input excitation. Thus, the approach could greatly reduce the analysis complexity. The effect of aliasing can effectively reduce by selecting a small sampling interval for the time domain excitation function. A sampling interval is acceptable as long as the amplitude of the Fourier transformed excitation is close to 0 over half of the sampling rate.

## Acknowledgments

This research was sponsored by Inner Mongolia Transportation Research Project (NJ-2014-X), Shanxi Transportation Research Project (2015-1-22) and National Natural Science Foundation of China (51208080). These supports are gratefully acknowledged.

## REFERENCES

- Al-Qadi, I.L., Xie, W., Elseifi, M.A., 2008. Frequency determination from vehicular loading time pulse to predict appropriate complex modulus in MEPDG. *Journal of the Association of Asphalt Paving Technologists* 77, 739–772.
- American Association of State Highway and Transportation officials (AASHTO), 2007. Standard Method of Test for Determining Dynamic Modulus of Hot-mix Asphalt (HMA). AASHTO TP 62-07. AASHTO, Washington DC.
- Bracewell, R.N., 2000. *The Fourier Transform and Its Applications*. McGraw-Hill, New York.
- Brigham, E.O., 1988. *The Fast Fourier Transform and Its Applications*. Prentice Hall, Upper Saddle River.

- Chehab, G.R., Kim, Y.R., Schapery, R.A., et al., 2003. Characterization of asphalt concrete in uniaxial tension using a viscoelastoplastic model. *Journal of Association of Asphalt Paving Technologists* 72, 315–355.
- Chen, E.Y.G., Pan, E., Green, R., 2009. Surface loading of a multilayered viscoelastic pavement: semianalytical solution. *Journal of Engineering Mechanics* 135 (6), 517–528.
- Cooley, J.W., Turkey, J.W., 1965. An algorithm for the machine calculation of complex Fourier series. *Mathematics of Computation* 19 (90), 297–301.
- Elseifi, M.A., Al-Qadi, I.L., Yoo, P.J., 2006. Viscoelastic modeling and field validation of flexible pavements. *Journal of Engineering Mechanics* 132 (2), 172–178.
- Gibson, N., Schwartz, C., Schapery, R.A., et al., 2003. Viscoelastic, viscoplastic, and damage modeling of asphalt concrete in unconfined compression. *Transportation Research Record* 1860, 3–15.
- Huang, Y., 2003. *Pavement Analysis and Design*. Prentice Hall, Upper Saddle River.
- Kim, J., Sholar, G.A., Kim, S., 2008. Determination of accurate creep compliance and relaxation modulus at a single temperature for viscoelastic solids. *Journal of Materials in Civil Engineering* 20 (2), 147–156.
- Luo, R., Lytton, R.L., 2010. Characterization of the tensile viscoelastic properties of an undamaged asphalt mixture. *Journal of Transportation Engineering* 136 (3), 173–180.
- Park, S.W., Kim, Y.R., 2001. Fitting Prony-series viscoelastic models with power-law presmoothing. *Journal of Materials in Civil Engineering* 13 (1), 26–32.
- Park, S.W., Schapery, R.A., 1999. Methods of interconversion between linear viscoelastic material functions. Part I: a numerical method based on Prony series. *International Journal of Solids and Structures* 36 (11), 1653–1675.
- Pellinen, T., Zofka, A., Marasteanu, M., et al., 2007. Asphalt mixture stiffness predictive models. *Journal of the Association of Asphalt Paving Technologists* 76, 575–625.
- Stearns, S.D., Hush, D.R., 2003. *Digital Signal Processing with Examples in Matlab*. CRC Press, Boca Raton.
- Tschoegl, N.W., 1989. *The Phenomenological Theory of Linear Viscoelastic Behavior: An Introduction*. Springer-Verlag, Berlin.
- Underwood, B.S., Kim, Y.R., Guddati, M.N., 2006. Characterization and performance prediction of ALF mixtures using a viscoelastoplastic continuum damage model. *Journal of the Association of Asphalt Paving Technologists* 75, 577–636.
- Wang, J., Birgisson, B., Roque, R., 2006. Effects of viscoelastic stress redistribution on the cracking performance of asphalt pavements. *Journal of Association of Asphalt Paving Technologists* 75, 637–675.
- Zhao, Y., Liu, H., Bai, L., et al., 2013. Characterization of linear viscoelastic behavior of asphalt concrete using a complex modulus model. *Journal of Materials in Civil Engineering* 25 (10), 1543–1548.
- Zhao, Y., Ni, Y., Wang, L., et al., 2014. Viscoelastic response solutions of multilayered asphalt pavements. *Journal of Engineering Mechanics* 140 (10), 401–408.